EPS-0785
Submitted to Pa 14 and Pl 3, 4, 11

Inclusive D^0 and $D^{*\pm}$ Production in Deep Inelastic ep Scattering at HERA

H1 Collaboration

Abstract

First results are presented on the inclusive D^0 and $D^{*\pm}$ production in deep inelastic electron proton scattering based on data taken with the H1 detector at the ep collider HERA in 1994. The D^0 is detected via its decay modes into $K^-\pi^+$ and $K^{*-}\pi^+ \rightarrow K_s^0\pi^-\pi^+$ while the D^{*+} is analyzed in the channel $D^{*+} \rightarrow D^0\pi^+_{slow} \rightarrow (K^-\pi^+)\pi^+_{slow}$. Preliminary results on the charm cross section in deep inelastic scattering for 10 GeV^2 $< Q^2 <$100 GeV^2 are given.

1 Introduction

The measurement of the charm production cross section in deep inelastic lepton nucleon scattering is of importance for the understanding of the parton densities in the nucleon [1]. According to early measurements of the EMC collaboration [2] the current picture of heavy quark production in leading order QCD is based on the *photon gluon fusion* process (fig. 1),

$$\gamma g \rightarrow c\bar{c}X, \tag{1}$$

where a gluon in the proton interacts with a photon emitted by the electron. Although this process is dominated by photoproduction where the interaction takes place on a quasireal photon target ($Q^2 \approx 0$, see [3] for preliminary results from H1) contributions from highly virtual photon exchange at large Q^2 are expected to be sizeable. Additional contributions due to fragmentation and gluon splitting, which is suppressed by heavy quark mass effects, are supposed to be small[4, 5]. Therefore, within this framework, charmed hadrons act as a probe for the gluon density in the nucleon. Furthermore, the data taken at HERA allows to look for non-pertubatively generated charm sea contributions in the proton to a much higher sensitivity than in Ref.[2]. Currently the kinematics and the luminosity of HERA do not allow to search for an intrinsic charm content of the proton [6], where the proton wave function fluctuates to a $|uudc\bar{c}\rangle$ state.

2 Data selection and analysis

The experiment is carried out using the H1 detector at the HERA storage ring at DESY. A detailed description of the detector can be found in ref. [7]. The data are collected during the 1994 running period where 27.6 GeV electrons (positrons) collided with 820 GeV protons, at a centre-of-mass energy of 300 GeV. The integrated luminosity is $\mathcal{L}_{int} = (2.97 \pm 0.04)pb^{-1}$.

The selection of deep inelastic scattering events requires the observation of a scattered electron with an energy of more than 13 GeV in the backward electromagnetic calorimeter of the H1 detector ($151^o < \Theta_e < 174^o$). Standard cuts are applied in order to ensure a good quality measurement of the electron candidate [8]. The kinematical variables x and Q^2 are calculated from the scattered electron.

The analysis is based on charged particles which have to be visible in the central tracker of the detector. Apart from the electron candidate at least 2 or 3 tracks, depending on the decay mode, have to be fitted to a common event vertex, which has to lie within 30 cm of the nominal interaction point in the beam direction. A minimum track length of 10 cm in the plane perpendicular to the beam direction is required for all charged tracks used for the D^0 reconstruction in the inclusive D^0 and D^{*+} analyses.

$D^0(1864)$ and $D^{*+}(2010)$ mesons are reconstructed to tag heavy quark production[1]. The D^0 is searched for in its decay modes

$$D^0 \rightarrow K^-\pi^+ \tag{2}$$

and

$$D^0 \rightarrow K^{*-}\pi^+ \rightarrow K^0_s\pi^-\pi^+\,, \tag{3}$$

[1]Henceforth, charge conjugate states are always implicitly included.

with the K_s^0 decaying into $\pi^+\pi^-$. K_s^0 candidates are defined by a pair of tracks with opposite charge fitted only to a secondary vertex having a minimal radial distance of 0.8 cm from the nominal beam spot. Further requirements applied to select good K_s^0 candidates are similar to those given in ref. [9].

The D^{*+} is detected in the channel

$$D^{*+} \to D^0 \pi^+_{slow} \to K^- \pi^+ \pi^+_{slow} \,. \tag{4}$$

Here use is made of the tight kinematical constraint for the decay of $D^{*+} \to D^0\pi^+_{slow}$. Due to the small mass difference between the D^{*+} and the D^0 mesons, the momentum of the soft pion (π_{slow}) in the D^{*+} rest frame is 39.6 MeV only. Therefore a better resolution is expected for the mass difference

$$\Delta m = m(D^0\pi^+_{slow}) - m(D^0) \tag{5}$$

rather than for the D^{*+} mass itself, whose width is dominated by the momentum resolution of the detector. In addition the combinatorial background is substantially reduced due to the smallness of the mass difference which is very close to the mass of the charged pion. No cut on the track length is applied in selecting the slow pion.

In addition to the reconstruction of the specific final states the general strategy in searching for charm induced events is based on the hard fragmentation of charmed hadrons [10]. To make use of this the analysis is performed in the γp system. In the naive quark parton model[2] (QPM) the ep interaction is described by the emission of a virtual photon from the electron which scatters off a quark from the nucleon. Thus the scattered current quark and the proton remnant are back to back in the γp system. For the kinematical region accessible at HERA the energy of the current quark in this picture is well estimated by the energy of the incoming proton in this hadronic centre of mass system. Analogue to the analyses performed by e^+e^- experiments the quantity

$$x_D = \left(\frac{|\vec{p}_D|}{|\vec{p}_p|} \right)_{\gamma p} \tag{6}$$

is defined for the D^0 in the γp system. Since this frame differs from the partonic centre of mass system in general, the observed x_D distribution does not compare directly to that obtained in $e^+e^- \to c\bar{c}$.

Furthermore an ordering O^+, O^-, O^0 of the visible particles is introduced according to

$$p_1^+ > p_2^+ > \ldots > p_n^+ \quad \text{and} \quad p_1^- > p_2^- > \ldots > p_m^- \tag{7}$$

for the charged particles and

$$p_i^0 > min(p_i^+, p_i^-) \tag{8}$$

for the K_s^0 candidates. By this procedure the fastest particle of a given charge in the γp system gets the order O^+, O^-, $O^0 = 1$ etc. The labeling O^+, O^-, O^0 will be subsequently

[2]This model is not really appropriate for the analysis. In case of the boson gluon fusion process (BGF) the $c\bar{c}$ CMS ($\hat{s}$) would be the correct one, which only becomes calculable after the reconstruction of the two jets. Due to acceptance and due to the behaviour of $d\sigma/d\hat{s}$ of the BGF cross section this reference frame can be reconstructed only for a small fraction of events.

related to O_K and O_π, according to the physical interpretation of the reconstructed particle in the analysis. It turns out that due to the hard fragmentation of charmed hadrons their decay products tend to be the leading particles of the events.

The effect of these quantities on the selection of charm events is demonstrated for the data in case of the D^{*+} analysis. In figure 2 the x_D distribution of the D^{*+} candidates, defined by 1.796 GeV$< m_{K\pi} <$ 1.936 GeV and 0.143 GeV$< m_{K\pi\pi} - m_{K\pi} <$0.147 GeV, is compared to the combinatorial background obtained from the intervals 1.796 GeV$< m_{K\pi} <$ 1.936 GeV and 0.170 GeV$< m_{K\pi\pi} - m_{K\pi} <$0.180 GeV without applying any further cuts to the data. The normalization of the background is obtained from the two body phase space factors of the different $m_{K\pi\pi} - m_{K\pi}$ intervals [3]. In the D^0 region a harder x_D spectrum is clearly observed. Evidently the requirement of a minimum x_D for the D^0 candidates reduces the combinatorial background of non charm induced events.

In figure 3 the correlation between the order O_K of the kaon candidate and the order O_π of the pion candidate for this decay mode is shown for the signal and background region as defined above. The definition of the kaon is obtained from the charge correlation with respect to the particle assumed to be the slow pion π_{slow} from the D^{*+} decay. As for the previous figure the background is normalized according to the phase space volumes. In the signal region a prominent peak is observed for those mass combinations where both particles are the leading particles ($O_K = O_\pi = 1$) of its charge. Thus the selection of leading particles according to (7,8) enhances the fraction of charm induced events further. Both, the x_D variable and the particle order are used in the subsequent analyses, where the cuts are chosen such that the reduction of the background inherent to the different decay channels is optimized.

2.1 $D^0 \to K^-\pi^+$

For each event the mass combination $m_{K\pi}$ of the leading particles, i.e. $O_K = O_\pi = 1$, is calculated. No particle identification is applied; each particle is assumed to be a kaon or a pion, thereby obtaining exactly two mass combinations per event. The fractional momentum in the γp system of the mass combinations has to satisfy $x_D > .35$. Additionally a momentum in the plane perpendicular to the beam direction of one of the particles of $p_T > 0.5$GeV is required while the other particle has to fulfil $p_T > 1.5$GeV. Finally a cut in the helicity angle Θ^*_K of the kaon in the D^0 rest frame with respect to the D^0 direction in the laboratory system of $-0.5 < \cos\Theta^*_K < 0.3$ is applied. The cut in the helicity angle reduces the combinatorial background from fragmentation, which peaks at large angles, significantly.

Figure 4 shows the mass distribution of the $m_{K\pi}$ combinations accepted after these cuts. Clear evidence for D^0 production is observed. A fit to the data of a Gaussian for the D^0 and an exponential background plus a Gaussian at low values of $m_{K\pi}$, which accounts for the contributions due to reflections from other D^0 decay modes and from

[3] This factor is simply given by the ratios of the integrals

$$\int_{\Delta m^{min}}^{\Delta m^{max}} d(\Delta m)\ \frac{\sqrt{((m_{K\pi}+\Delta m)^2-(m_{K\pi}+m_\pi)^2)\cdot((m_{K\pi}+\Delta m)^2-(m_{K\pi}-m_\pi)^2)}}{2(m_{K\pi}+\Delta m)^3}$$

for the different Δm intervals.

D^+ decay, yields 198±33 mass combinations in the D^0 peak. The width of the signal $\sigma(m_{D^0}) = (40 \pm 7)$ MeV is in agreement with the Monte Carlo expectation of (36 ± 5) MeV. Due to the tight cut on the helicity angle Θ^*_K the expected contribution to the signal of the wrong K, π assignment to the tracks is $50 \pm 3\%$. After subtraction of these wrong mass assignments a net signal of (99 ± 18) D^0's is observed. A small shift for the reconstructed D^0 mass of $\Delta m_{D^0} = (16 \pm 8)$ MeV with respect to the nominal value is observed due to the cut in the helicity angle, which leads to a non-Gaussian contribution from the wrong K, π assignment to the tracks in the signal region.

2.2 $D^0 \to K^{*-}\pi^+ \to K^0_s\pi^-\pi^+$

For each event having a good K^0_S candidate with a transverse momentum $p_T^{K^0_S} > 0.5$GeV, a decay length $l_d^{K^0_S} > 8\,cm$ and a apparent proper time of $60\,ps < \tau_{K^0_S} < 380\,ps$ all mass combinations $m(K^0_s\pi^-)$ are calculated. The combinations fulfilling

$$|m(K^0_s\pi^-) - m_{K^*}| < 0.1\text{GeV} \tag{9}$$

and

$$|\cos\Theta^*_{K,K^*}| < 0.2 \tag{10}$$

are considered as K^{*-} candidates. Here $\cos\Theta^*_{K,K^*}$ denotes the angle of the kaon in the K^* rest frame with respect to the K^* direction in the laboratory frame. The cut in this angle accounts for the spin of the K^*. The K^{*-} candidates are subsequently combined with all oppositely charged tracks having transverse momenta $p_T^\pi > 0.15$GeV to form D^0 candidates. The angle $\Theta^*_{K^*,D^0}$ of the K^* in the D^0 rest frame with respect to the laboratory frame has to fulfil $|\cos\Theta^*_{K^*,D^0}| < .85$, which reduces the combinatorial background from the fragmentation.

Figure 5 shows the mass distribution of all $m(K^0_s\pi^-\pi^+)$ mass combinations having a fractional momentum in the γp system of $x_D > .25$ and a transverse momentum in the laboratory frame $p_T^{D^0} > 2$GeV. Clear evidence for a signal at the D^0 mass is observed. A fit of a Gaussian plus an exponential to the data yields a net signal of 49 ± 10 D^0's. The peak position at $m_{D^0} = 1.878 \pm 0.006$ GeV is in reasonable agreement with the nominal value. The width of the distribution of $\sigma_{D^0} = 24 \pm 4$ MeV agrees well with the Monte Carlo expectation of 27 MeV.

2.3 $D^{*+} \to D^0\pi^+_{slow} \to K^-\pi^+\pi^+_{slow}$

Since this analysis profits from the effects of the tight mass constraint of the decay $D^{*+} \to D^0\pi^+$ the criteria for the particle and D^0 candidate selection may be looser compared to the inclusive D^0 analyses. Only particles having a transverse momentum of $p_T > 0.25$GeV in the laboratory frame are considered for the reconstruction of D^0 candidates.

According to figure 3 the mass combinations $m_{K\pi}$ fulfilling the requirements

$$(O_{K,\pi} = 1 \wedge O_{\pi,K} \leq 2) \tag{11}$$

are calculated for each event. As in the previous analyses no particle identification is applied so that each particle is assumed to be a kaon or a pion. The fractional momentum in the γp system of each of the mass combinations has to satisfy $x_D > .25$ to be accepted. At small x the selection based on leading particles and large x_D in the γp system favours D^0 candidates pointing backward in the laboratory frame, since they are closest to the QPM expectation, by which the selection has been motivated. Since the background in the D^{*+} analysis is already suppressed significantly due to phase space, also those $m_{K\pi}$ mass combinations are excepted, which satisfy $p_T(K^-\pi^+) > 3\mathrm{GeV}$, irrespectively of O_K, O_π and x_D. By this alternative criterion especially the D^{*+}'s going in forward direction at small x will survive and thereby the overall efficiency is increased. The $m(K^-\pi^+)$ combinations within $\pm 70\,\mathrm{MeV}$ of the nominal D^0 mass of $1.865\,\mathrm{GeV}$ are combined with an additional charged track which has a transverse momentum greater than 0.1 GeV and a charge opposite to that of the kaon candidate.

Figure 6 shows the distribution of the mass difference for the accepted D^{*+}-candidates. Clear evidence for D^{*+} production is found in the signal region, defined as a $\pm 2.5\,\mathrm{MeV}$ window around the expected mass difference of 145.4 MeV. A fit of a Gaussian plus a background term according to the two body phase space yields a signal of 99 ± 12 D^{*+}'s. The peak position at $\Delta m = 145.5 \pm 0.14$ MeV as well as the width of the Gaussian of $\sigma = (1.1 \pm .2)$ MeV agrees well with the Monte Carlo expectation. According to Monte Carlo studies this signal contains contaminations due to reflections from D^0 decay modes different from $D^0 \rightarrow K^-\pi^+$ of $(4.9 \pm 1.7)\%$. No enhancement is observed in the background obtained from mass combinations with $m_{K\pi} > 2\,\mathrm{GeV}$ as shown by the histogram in fig 6[4].

Figure 7 shows the mass distribution of the $m_{K\pi}$ combinations for events in the Δm signal region. The histogram shows the background expectation from the region $0.170\mathrm{GeV} < \Delta \mathrm{m} < 0.180\mathrm{GeV}$ scaled by the two body phase space factors. It describes well the $K^-\pi^+$ mass distribution for $m_{K\pi} > 2\,\mathrm{GeV}$. Below 2 GeV large differences are observed in the $m_{K\pi}$ distribution from the Δm signal region as compared to the background expectation which are completely due to contributions where both particles originate from the decay $D^{*+} \rightarrow D^0\pi^+_{slow}$. Clear signals are observed for the D^0 as well as for the "S^0" from the decay $D^0 \rightarrow K^-\pi^+\pi^0$ where the π^0 is not detected. The width of the Gaussian of the D^0 of $\sigma_{D^0} = (37 \pm 7)$ MeV is again in agreement with the Monte Carlo expectation of 35 MeV.

3 Results

In the following the results of the independent analyses of the decay modes $D^0 \rightarrow K^-\pi^+$ and $D^{*+} \rightarrow D^0\pi^+$ (and their charge conjugates) will be considered. The production cross section in ep collisions for the experimentally accessible ranges of $Q^2 > 10\mathrm{GeV}^2$ and $|\ \eta_D\ | \leq 1.25$ is calculated from the observed numbers N_{obs} of D^0 and D^{*+} candidates, according to the formula

$$\sigma(ep \rightarrow DX) = \frac{N_{obs}(Q^2, \eta_D)}{\mathcal{L}_{int} \cdot B \cdot \epsilon_{tot}}, \tag{12}$$

where D stands for D^0 and D^{*+} and their charge conjugates. Here $\eta(D)$ denotes the pseudorapidity of the D^0 and D^{*+}, respectively, while $\mathcal{L}_{int}$, B and ϵ_{tot} refers to the in-

[4]Since the selection is mainly based on the leading particles in the γp system, the background behaviour cannot be studied by the like sign $K\pi$ mass combinations.

tegrated luminosity, the branching ratios $B = B(D^0 \to K^-\pi^+) = 0.0401 \pm 0.0014$ and $B = B(D^{*+} \to D^0\pi^+) \cdot B(D^0 \to K^-\pi^+) = 0.0273 \pm 0.0011$ [11], respectively, and the total efficiency. A Monte Carlo simulation is used to determine the efficiency for the selection cuts and the geometrical acceptance of the detector. The number of observed events, N_{obs}, is obtained from the fits to the spectra.

Preliminary ep production cross sections of

$$\sigma(ep \to D^0 X) = (7.0 \pm 1.3 \pm 1.5)\, nb \tag{13}$$

and

$$\sigma(ep \to D^{*+} X) = (2.9 \pm 0.3 \pm 0.4)\, nb \tag{14}$$

are obtained in the kinematical region described above. The errors refer to the statistical and the experimental systematics. The statistical error includes the uncertainty due to the limited Monte Carlo statistics. The experimental systematics are summarized in table 1. For the D^0 cross section the major systematic uncertainty comes from the shape of the reflections below the D^0 mass while the uncertainty in the $D^{*\pm}$ cross section is dominated by the track reconstruction efficiency of the slow pion. The different contributions to the experimental systematic uncertainties are added in quadrature resulting in an overall relative error of 22% and 13% for the inclusive D^0 and D^{*+} cross section, respectively.

From these cross sections the ratio

$$\frac{\sigma(ep \to D^{*\pm} X)}{\sigma(ep \to D^0 X)} = 0.41 \pm 0.09 \pm 0.10 \tag{15}$$

is determined, which agrees well with

$$\frac{\langle n_{D^{*+}} \rangle}{\langle n_{D^0} \rangle} = 0.50 \pm 0.05 \tag{16}$$

from e^+e^- data. Here $\langle n_{D^{*+}} \rangle$ and $\langle n_{D^0} \rangle$ are the weighted world averages calculated from Ref. [5, 12].

Assuming that charmed hadrons are directly produced either from charm or bottom quarks originating from the hard subprocess together with the assumption of $B(c \to D) = B(b \to D)$, justified by the recent measurement of OPAL [5], the world averages on $\langle n_{D^0} \rangle$ and $\langle n_{D^{*+}} \rangle$ can be turned into the branching ratio of charm quarks into D^0 and D^{*+} of

$$B(c \to D^0) = 0.50 \pm 0.04 \tag{17}$$

and

$$B(c \to D^{*+}) = 0.248 \pm 0.014\,. \tag{18}$$

This leads to a preliminary total charm ep production cross section of

$$\sigma(ep \to c\bar{c}X) = \zeta \cdot \frac{\sigma(ep \to D^0 X)}{B(c \to D^0) \cdot (1 + \xi)} = (10.2 \pm 2.0 \pm 2.0 \pm 2.6)\, nb \tag{19}$$

from the inclusive D^0 production and

$$\sigma(ep \to c\bar{c}X) = \zeta \cdot \frac{\sigma(ep \to D^{*\pm} X)}{B(c \to D^{*+}) \cdot (1 + \xi)} = (8.3 \pm 0.9 \pm 1.2 \pm 2.1)\, nb \tag{20}$$

from the inclusive D^{*+} production for $Q^2 \geq 10\mathrm{GeV}^2$ and $|\eta_D| \leq 1.25$. The errors refer to the statistical, the experimental systematic, and the uncertainty due to model dependencies. Here $\zeta = 0.77 \pm 0.01$ denotes the correction factor, which accounts for the probability, that both charm quarks fall into the η acceptance and $\xi = 0.06 \pm 0.02$ is the correction due contributions from fragmentation and bottom production. Both correction factors are determined by Monte Carlo methods. The contribution of the fragmentation found by simulation agrees well with the expectation from e^+e^- measurements [4, 5]. The cross sections are restricted to a limited $|\eta_D|$ region because the extrapolation beyond the experimental acceptance may introduce additional uncertainties due to the unknown behaviour of the parton densities. According to Monte Carlo studies the pseudorapidity of the D meson coincides with the pseudorapidity of the charm quark with $\sigma(\eta_D - \eta_c) \approx 0.1$.

The model uncertainties in the calculation of the cross section originate mainly from the choice of the parton densities, the charm quark mass and the order used in the QCD calculation of the BGF matrix element. All numbers are based on simulations using the LEPTO 6.1 generator program assuming the MRS(H) parametrization of the parton densities in the proton and neglecting the mass of the charm quark. This model uses leading order calculations of the QCD matrix elements. The influence of the parton densities has been studied using the MRSD0' [13] parametrization, which reduces the acceptance in the $|\eta|$ range by 5%, and using the GRV-HO [14] parametrization,which leads to an increase of the acceptance in the $|\eta|$ range by 5%. From the x_D distribution, which is a measure of the dynamics of the hard subprocess, a relative uncertainty in the cross section due to charm quark mass effects and higher order corrections of 20 % is estimated. The combined systematic error from these model dependencies is estimated to 25 % and is quoted separately in eqns. (19,20).

4 Conclusions

First results on the inclusive D^0 and D^{*+} meson production in deep inelastic ep scattering have been presented. Preliminary inclusive cross sections of $\sigma(ep \to D^0 X) = (7.0 \pm 1.3 \pm 1.5)\,nb$ and $\sigma(ep \to D^{*+}X) = (2.9 \pm 0.3 \pm 0.4)\,nb$ at $Q^2 \geq 10\mathrm{GeV}^2$ and $|\eta_D| < 1.25$ are obtained. The observed ratio $\sigma(ep \to D^{*\pm}X)/\sigma(ep \to D^0 X) = 0.41 \pm 0.09 \pm 0.10$ agrees well with the expectation from e^+e^-. For the kinematical region $Q^2 \geq 10\mathrm{GeV}^2$ and $|\eta_D| < 1.25$ a preliminary charm production cross section of $\sigma(ep \to c\bar{c}X) = (10.2 \pm 2.0 \pm 2.0 \pm 2.6)\,nb$ from the D^0 analysis and $\sigma(ep \to c\bar{c}X) = (8.3 \pm 0.9 \pm 1.2 \pm 2.1)\,nb$ from the D^{*+} analysis has been derived.

Acknowledgments

We gratefully acknowledge the efforts of the HERA machine group for high-luminosity running, the DESY computer centre, and the DESY directorate for their support. The non-DESY members of the collaboration wish to thank the DESY directorate for the hospitality extended to them while working at DESY.

References

[1] A. Ali *et al.,* Proc. of the HERA Workshop, DESY, Hamburg, Vol. 1 (1988), 393
A. Ali and D. Wyler, Proc. of the Workshop "Physics at HERA", DESY, Hamburg, Vol. 2 (1991), 667 (and references therein)
M.A.G. Aivazis et al., Phys. Rev. D 50 (1994) 3085, Phys. Rev. D 50 (1994) 3102
S. Riemersma, J. Smith, W.L. van Neerven, Phys. Lett. B 347 (1995) 143

[2] EMC Collaboration J.J. Aubert *et al.,* Nucl. Phys. B 213 (1983) 31

[3] "Photoproduction of $D^{*\pm}$ Mesons in Electron Proton Collisions at HERA", H1 Coll., contributed paper EPS-0467 to this conference

[4] this can be inferred from the J/Ψ production at LEP: L3 Collaboration, O. Adriani et al., Phys. Lett. B 288 (1992) 412.

[5] R. Akers *et al.* (OPAL Coll), CERN PPE 94/217 (1994)

[6] S.J. Brodsky et al., Phys. Lett. 93 B (1980) 451, Phsy. Rev. D 23 (1981) 2745
G.A. Schuler, Nucl.Phys. B299 (1988), 21
G. Ingelman, L. Jönsson, and M. Nyberg, DESY 92-178 (1992)

[7] H1 Collaboration, I. Abt *et al.*, "The H1 Detector at HERA," DESY 93-103 (1993)

[8] H1 Collaboration, T. Ahmed *et al.,* Nucl. Phys. B 439 (1995) 471

[9] " Production of K_s^0 in Photoproduction and Deep-Inelastic Scattering at HERA", H1 Coll., contributed paper EPS-0479 to this conference

[10] Particle Data Group, M.Aguilar-Benitez *et al.*, Phys. Rev. D50 (1994), 1333 (and references therein)

[11] Particle Data Group, M.Aguilar-Benitez *et al.*, Phys. Rev. D50 (1994), 1171

[12] Particle Data Group, M.Aguilar-Benitez *et al.*, Phys. Rev. D50 (1994), 1331 (and references therein)

[13] A.D. Martin, R.G. Roberts, and W.J. Stirling, Phys.Lett. B306 (1993), 145

[14] M. Glück, E. Reya, and A. Vogt, Z. Phys. C 53 (1992) 127

[15] A.D. Martin, R.G. Roberts, and W.J. Stirling, RAL-94-055 (1994)

	Experimental systematic uncertainties	
	$D^0 \to K^-\pi^+$	$D^{*+} \to K^-\pi^+\pi^+_{slow}$
fragmentation & gluon splitting	0.02	0.02
charm fragmentation function	0.05	0.05
$B(D^0 \to K^-\pi^+)$	0.04	0.04
$B(D^{*+} \to D^0\pi^+_s)$	-	0.02
reflections	0.20	0.03
wrong $K\pi$ assignment	0.05	-
$K\pi$ track efficiency	0.05	0.05
π_{slow} track efficiency	-	0.10
luminosity	0.02	0.02
γp contribution	<0.02	<0.02
total	0.22	0.14

Table 1: Summary of the systematic experimental uncertainties

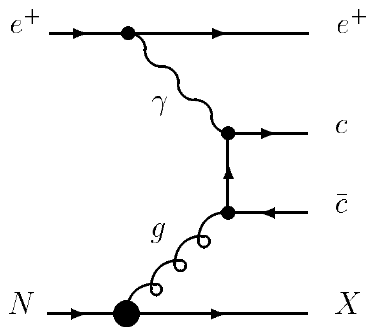

Figure 1: Feynman diagrams for the production of heavy quarks in deep inelastic lepton nucleon scattering.

H1 preliminary

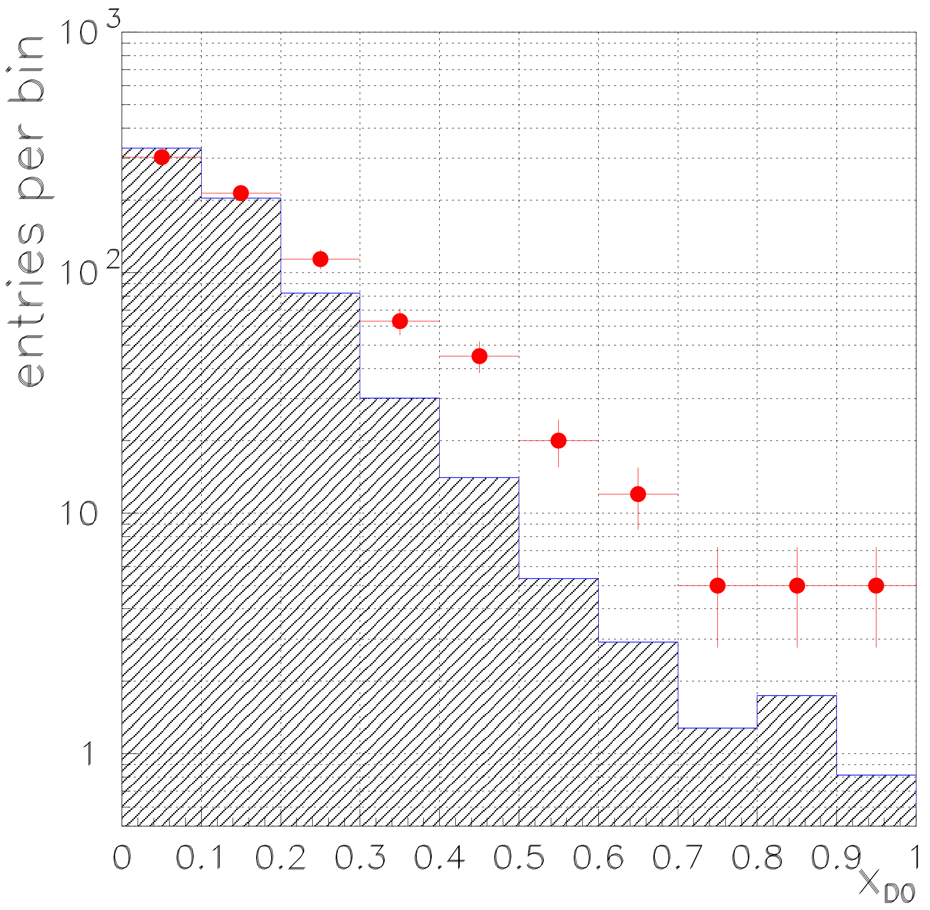

Figure 2: Distribution of the fractional momentum x_D of the D^0 candidate with respect to the incoming proton momentum in the γp system (data points) compared to the combinatorial background (hatched histogram) as observed in the data. The definition of the signal and the background region is given in the text.

H1 preliminary

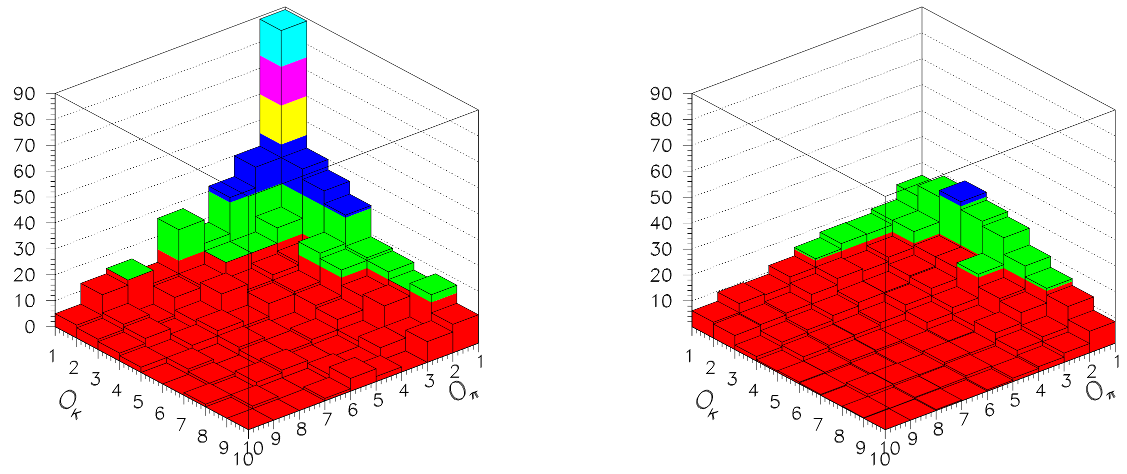

a) Signal Region

b)Background Region

Figure 3: Correlation of the order O_K and the order O_π in the γp frame a) in the signal region and b) for the combinatorial background as observed in the data. The kaon is defined by the charge correlation to the π_{slow} candidate. The definition of the signal and the background region is given in the text. The background is normalized according to the two body phase space volume. The leading particles of a given charge have $O = 1$.

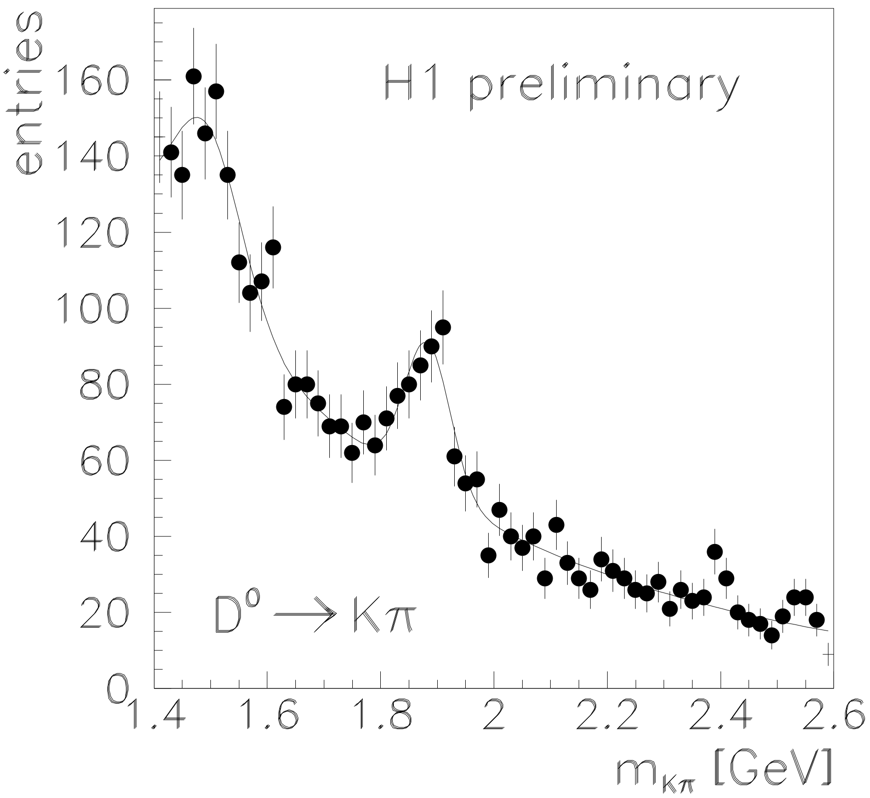

Figure 4: $K^-\pi^+$ mass distribution. The solid line is a fit of a Gaussian for the D^0 signal plus a exponential background term plus a Gaussian for low $m_{K\pi}$ values to the data. the second Gaussian accounts for the contribution due to reflections from other D^0 decay modes and from D^+ decay.

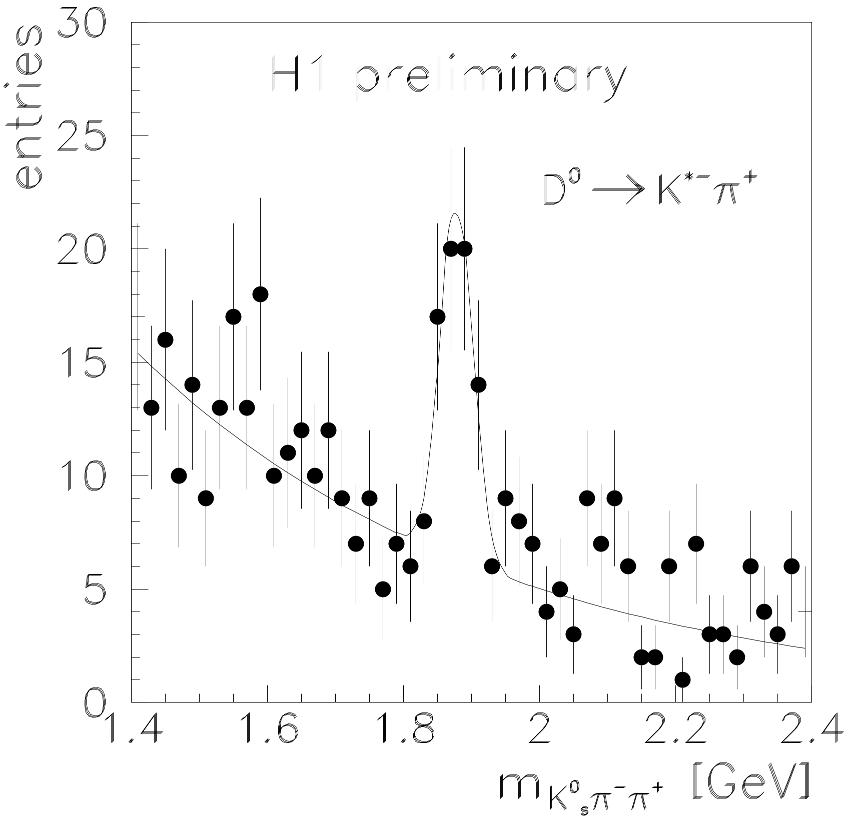

Figure 5: $K_s^0\pi^-\pi^+$ mass distribution fulfilling the K^{*-} constraints. The solid line is a fit of a Gaussian for the D^0 signal plus a exponential background term to the data.

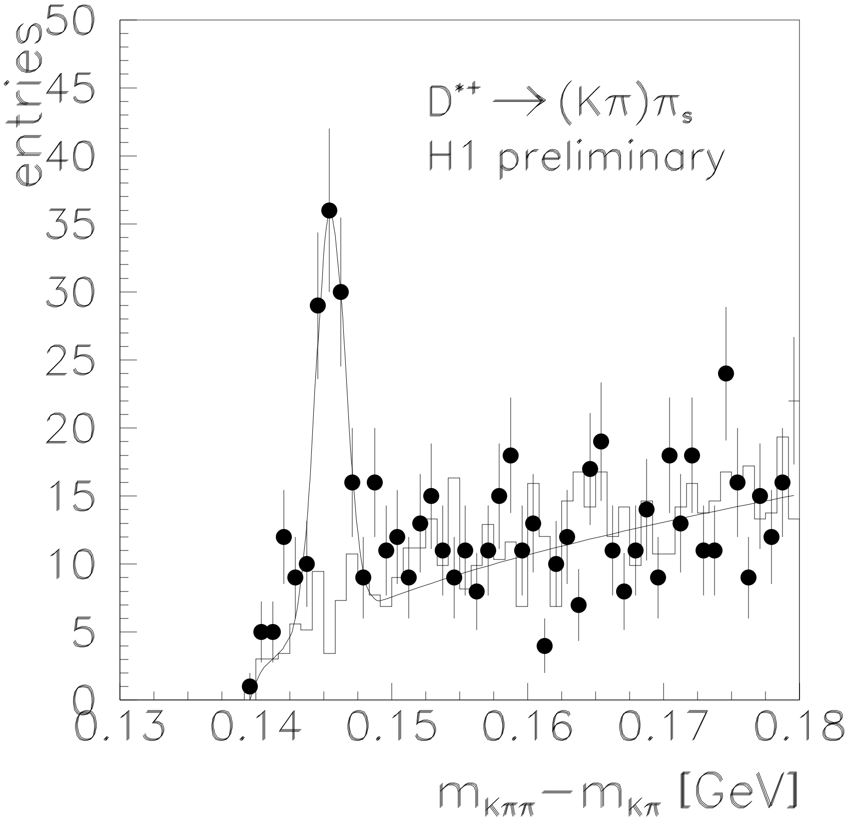

Figure 6: Distribution of the mass difference $\Delta m = m(K^-\pi^+\pi^+_{slow}) - m(K^-\pi^+)$ for deep inelastic scattering events. The data points are obtained from the $m(K^-\pi^+)$ mass combinations within an interval of 70 MeV around the nominal D^0 mass. The histogram shows the background expectation, which is obtained from the high mass sideband $2.0\mathrm{GeV} \leq \mathrm{m}(\mathrm{K}^-\pi^+) \leq 2.6\mathrm{GeV}$, normalized to the region $0.170\mathrm{GeV} \leq \Delta\mathrm{m} \leq 0.180\mathrm{GeV}$. The solid line is a fit of a Gaussian plus the two body phase space distribution to the data.

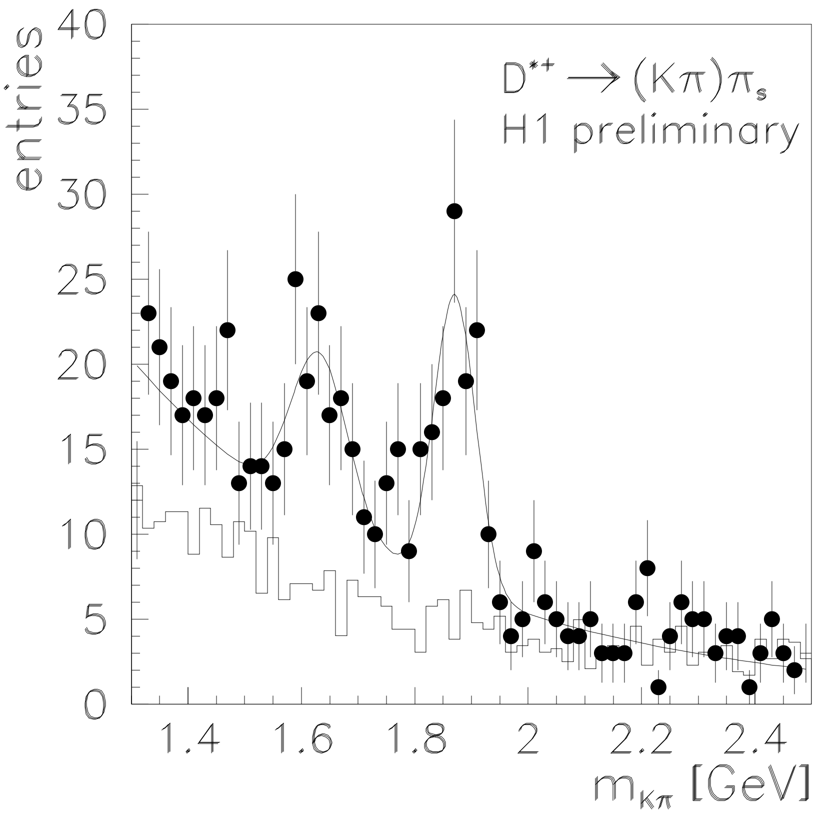

Figure 7: $K^-\pi^+$ mass distribution for candidates in the D^{*+} region $0.143\mathrm{GeV} \leq \Delta\mathrm{m} \leq 0.148\mathrm{GeV}$. The histogram shows the background expectation from the region $0.170\mathrm{GeV} \leq \Delta\mathrm{m} \leq 0.180\mathrm{GeV}$, normalized by the two body phase space factors according to the Δm intervals. The solid line represents the fit of two Gaussians for the D^0 and S^0 plus an exponential to the data.